



## Review article

# Metabolic switch during adipogenesis: From branched chain amino acid catabolism to lipid synthesis<sup>☆</sup>



Anna Halama<sup>a, b, 1</sup>, Marion Horsch<sup>a</sup>, Gabriele Kastenmüller<sup>c</sup>, Gabriele Möller<sup>a</sup>, Pankaj Kumar<sup>b</sup>, Cornelia Prehn<sup>a</sup>, Helmut Laumen<sup>d</sup>, Hans Hauner<sup>d</sup>, Martin Hrabě de Angelis<sup>a, e, f</sup>, Johannes Beckers<sup>a, e, f</sup>, Karsten Suhre<sup>b</sup>, Jerzy Adamski<sup>a, e, f, \*</sup>

<sup>a</sup> Institute of Experimental Genetics, Genome Analysis Center, Helmholtz Zentrum München, German Research Center for Environmental Health, Neuherberg, Germany

<sup>b</sup> Department of Physiology and Biophysics, Weill Cornell Medical College – Qatar, Doha, Qatar

<sup>c</sup> Institute of Bioinformatics and Systems Biology, Helmholtz Zentrum München, German Research Center for Environmental Health, Neuherberg, Germany

<sup>d</sup> Else Kröner-Fresenius-Centre for Nutritional Medicine, Klinikum Rechts der Isar, Technical University München, München, Germany

<sup>e</sup> German Center for Diabetes Research, Neuherberg, Germany

<sup>f</sup> Lehrstuhl für Experimentelle Genetik, Technische Universität München, Freising-Weihenstephan, Germany

## ARTICLE INFO

## Article history:

Received 10 May 2015

Received in revised form

13 September 2015

Accepted 15 September 2015

Available online 25 September 2015

## Keywords:

Adipogenesis

Obesity

Metabolomics

Metabolic pathways

Phosphatidylcholines

Fatty acids

Glycerophospholipids

Branched chain amino acids

## ABSTRACT

Fat cell metabolism has an impact on body homeostasis and its proper function. Nevertheless, the knowledge about simultaneous metabolic processes, which occur during adipogenesis and in mature adipocytes, is limited. Identification of key metabolic events associated with fat cell metabolism could be beneficial in the field of novel drug development, drug repurposing, as well as for the discovery of patterns predicting obesity risk. The main objective of our work was to provide comprehensive characterization of metabolic processes occurring during adipogenesis and in mature adipocytes. In order to globally determine crucial metabolic pathways involved in fat cell metabolism, metabolomics and transcriptomics approaches were applied. We observed significantly regulated metabolites correlating with significantly regulated genes at different stages of adipogenesis. We identified the synthesis of phosphatidylcholines, the metabolism of even and odd chain fatty acids, as well as the catabolism of branched chain amino acids (BCAA; leucine, isoleucine and valine) as key regulated pathways. Our further analysis led to identification of an enzymatic switch comprising the enzymes Hmgcs2 (3-hydroxy-3-methylglutaryl-CoA synthase) and Auh (AU RNA binding protein/enoyl-CoA hydratase) which connects leucine degradation with cholesterol synthesis. In addition, propionyl-CoA, a product of isoleucine degradation, was identified as a putative substrate for odd chain fatty acid synthesis. The uncovered crosstalks between BCAA and lipid metabolism during adipogenesis might contribute to the understanding of molecular mechanisms of obesity and have potential implications in obesity prediction.

© 2015 Elsevier Inc. All rights reserved.

## Contents

1. Introduction .....	94
2. Materials and methods .....	94
2.1. 3T3-L1 Preadipocyte culturing and differentiation into adipocytes .....	94
2.2. Cell harvesting and medium sampling .....	95
2.2.1. Medium sampling and cell harvesting for metabolomics .....	95
2.2.2. Harvesting of cells for Western blotting .....	95

<sup>☆</sup> Reviewer may access the dataset anonymously at: <http://www.ncbi.nlm.nih.gov/geo/query/acc.cgi?token=yzojmymupytbyj&acc=GSE34150>.

\* Corresponding author. Helmholtz Zentrum München, German Research Center for Environmental Health, Institute of Experimental Genetics, Genome Analysis Center, Ingolstaedter Landstrasse 1, 85764, Neuherberg, Germany.

E-mail address: [adamski@helmholtz-muenchen.de](mailto:adamski@helmholtz-muenchen.de) (J. Adamski).

<sup>1</sup> Present address of AH is in Weill Cornell Medical College – Qatar.

2.2.3. Harvesting of cells for RNA extraction .....	95
2.3. Oil red O assay .....	95
2.4. RNA isolation, quantitative real-time PCR (qPCR), and gene expression profiling .....	95
2.5. Western blotting .....	96
2.6. Metabolomics measurement .....	96
3. Results .....	96
3.1. Metabolomics combined with transcriptomics: a comprehensive tool to study adipogenesis .....	96
3.2. Branched chain amino acid metabolism is strongly regulated during adipogenesis .....	99
3.3. Leucine degradation products are linked to cholesterol biosynthesis .....	99
3.4. Interlink between isoleucine degradation and odd chain fatty acid synthesis .....	101
4. Discussion .....	101
Acknowledgements .....	105
Supplementary data .....	106
References .....	106

## 1. Introduction

Obesity has been identified as a major risk factor for chronic diseases, such as cardiovascular disease, hypertension, dyslipidemia, hyperglycemia [1], type 2 diabetes, insulin resistance [2,3], and some types of cancer [4] including colon [5], breast [6] and prostate cancer [7], as well as an increased risk of premature death [8]. Thus, identification of markers predicting the risk of obesity as well as determination of drug targets could strongly benefit the health system. Studies on obesity have recognized several factors including genetic background [9], interplay between environment and genetics [10] as well as epigenetic mechanisms [11] to be associated with this multifactorial disorder. Further understanding of obesity and its co-morbidities could be provided by metabolomics, enabling a global overview on metabolic processes in the body, which simultaneously reflect the sum of gene expression, protein abundance, and environmental influence [12]. Lately, metabolomics applied to a human cohort for the investigation of the metabolic difference between obese and lean individuals revealed a possible origin of insulin resistance associated with obesity [13]. This study highlighted that an increase in plasma branched chain amino acid (BCAA) concentrations is a hallmark of adult obese individuals. The BCAAs have also been shown to contribute to obesity-associated insulin resistance [13]. In contrast, a study with obese children and children with type 2 diabetes indicated down-regulation in the plasma BCAA levels compared to healthy lean subjects [14,15]. Clearly, BCAA metabolism is altered in obesity; however, our current understanding how it is regulated and cross-linked to other pathways has not been fully elucidated.

This discrepancy could be associated with the dynamics of fat cell turnover [16]. It has been shown that the number of fat cells is settled during childhood and adolescence and is constant in adulthood of lean and obese individuals, independent of weight loss or gain [16]. Consequently, differences in fat cell fates of children/adolescents and adults could have direct impact on the diverse patterns in their metabolism, since adipocytes are involved in synthesis and secretion of several hormones [17] and thereby contribute to energy homeostasis [18]. Thus, an increased adipocyte size and/or number results in an increase of molecules released by adipocytes including e.g. adipokines, free fatty acids, and inflammatory mediators, which affect other tissues such as liver, muscle, or neural connections leading to co-morbidities of obesity [3,19].

Exploration of ongoing metabolic changes during adipogenic cell differentiation and in mature adipocytes might facilitate the identification of metabolic pathways and biomarkers useful for

obesity prediction and identification of novel drug targets.

However, possibilities to perform mechanistic and functional analyses in the whole organism are limited, and therefore we and others applied analyses on the molecular basis of adipogenesis in cell culture.

The adipogenic cell differentiation process has been already investigated with different omics tools, particularly transcriptomics [20–22], proteomics [23–25], and recently metabolomics [26]. However, more specific insight into the regulation of metabolic pathways can be gained by combining different omics technologies. For example, metabolomics and genomics have already been successfully applied by us in human studies (mGWAS) [12,27–29] and generated new hypotheses for biomedical and pharmaceutical research [29].

In the present study we combined for the first time metabolomics and transcriptomics in order to provide a comprehensive overview on adipogenesis and fat cell metabolism using the murine 3T3-L1 cell culture model. Our main goal was to reveal interconnected pathways and biomarkers for adipogenesis to further facilitate the identification of targets useful in prediction and therapies of obesity.

We found associations between BCAA degradation products and intermediates of the cholesterol synthesis as well as even and odd chain fatty acid metabolism. The metabolic signatures of adipogenesis observed in our study further support the BCAAs as important players in fat metabolism and highlight odd-chain fatty acids and glycerophospholipids as novel biomarkers of adipogenesis. Furthermore, differences in BCAA metabolism between children/adolescents and adults observed previously [13–15], might be associated with the process of adipogenesis [16]. Therefore, a decreased BCAA level in children might suggest increased formation of fat cells and simultaneously serve as a biomarker for obesity prediction. The metabolic pathways of BCAA catabolism and glycerophospholipid synthesis should be considered as potential drug targets preventing obesity.

## 2. Materials and methods

### 2.1. 3T3-L1 Preadipocyte culturing and differentiation into adipocytes

3T3-L1 cells (murine preadipocytes) obtained from the American Type Culture Collection (ATCC) were grown at 37 °C in a 5% CO<sub>2</sub> humidified atmosphere in growth medium DMEM (High Glucose (4.5 g/L); PAA Laboratories), supplemented with 10% fetal bovine serum (FBS; PAA Laboratories), 100 IU/mL penicillin, and 100 mg/mL streptomycin (Invitrogen).

Cells were seeded out in 6-well plates at a density of  $8 \times 10^4$  cells/well and were grown for 2 days until they reached confluence. Two days after cells reached confluence (specified as day 0 of adipogenesis or preadipocyte status) adipogenic cell differentiation was induced by cells treatment for four days with a mixture containing growth medium, insulin (10 mg/mL; Sigma), dexamethasone (1  $\mu$ M, Sigma), and 3-isobutyl-1-methylxanthine (IBMX; 0.5 mM; Sigma). After four days of differentiation, adipocyte maturation was initiated by cultivating the cells from thereon in growth medium containing only insulin (10 mg/mL) for the remaining maturation process. The media were exchanged every 48 h with fresh media modified as described above. The cells were maintained for 18 days and samples (cells and their conditioned media separately) were collected at 8 different time points (day 0, 2, 4, 6, 8, 10, 14, and 18).

## 2.2. Cell harvesting and medium sampling

### 2.2.1. Medium sampling and cell harvesting for metabolomics

The conditioned medium was removed from the cells and transferred to 1.5 mL reaction tubes, snap-frozen in liquid nitrogen, and stored at  $-80^\circ\text{C}$  until further processing.

In order to determine the best method for cell harvesting and metabolite extraction, we examined two harvesting methods including trypsinization and scraping, followed by extraction with three different extraction solvents including water, 40% MeOH and 80% MeOH.

For cell harvesting by trypsinization culture medium was removed, cells were washed once with 2 mL of PBS and incubated with 0.5 mL/well of trypsin (Gibco) for 1 min at  $37^\circ\text{C}$ . To each well 1.5 mL of medium was added, cells were suspended, transferred to 1.5 mL reaction tubes and centrifuged. The supernatant was removed and cells were washed twice with 1 mL pre-warmed PBS buffer ( $37^\circ\text{C}$ ). After PBS was aspirated, 350  $\mu$ L of extraction solvent (either water, 40% MeOH, or 80% MeOH) were added and samples were snap-frozen in liquid nitrogen and stored at  $-80^\circ\text{C}$  until further processing.

For cell harvesting by scraping culture medium was aspirated and cells were washed twice with 2 mL pre-warmed PBS buffer ( $37^\circ\text{C}$ ). After PBS was aspirated, 350  $\mu$ L of extraction solvent (either water, 40% MeOH, or 80% MeOH) were added and cells were scraped off the well bottom in extraction solvent. The suspension (cells in extraction solvent) was transferred to 1.5 mL reaction tubes, snap-frozen in liquid nitrogen and stored at  $-80^\circ\text{C}$  until further processing.

After having compared the metabolic profiles of cells harvested by trypsinization and by scraping followed by extraction with either water, 40% MeOH or 80% MeOH (Suppl. Fig. 1), we found scraping combined with the 80% methanol extraction to result in the best detection of metabolites over all metabolite classes (Suppl. Fig. 1). This sampling/extraction technique was from then on applied to all cells that were sampled for metabolomics measurements in this study. Samples for metabolomics studies were prepared in triplicates in three independent experiments.

### 2.2.2. Harvesting of cells for Western blotting

Culture medium was removed, cells were washed once with 2 mL PBS and then scraped off the well bottom with 300  $\mu$ L lysis buffer (Cell Signalling) supplemented with protease and phosphatase inhibitors (Roche) as well as phenylmethanesulfonyl fluoride (PMSF), a serine protease inhibitor. Cell lysates were stored at  $-80^\circ\text{C}$  until use. Samples for Western blotting were prepared in three independent experiments.

### 2.2.3. Harvesting of cells for RNA extraction

Culture medium was removed, cells were washed once with 2 mL PBS followed by addition of Trizol (0.5 mL/well) and cells were scraped off the well. Cell/Trizol suspensions were transferred to 1.5 mL reaction tubes and stored at  $-80^\circ\text{C}$  until further processing. Samples for RNA extraction were prepared in three independent experiments.

## 2.3. Oil red O assay

At each harvesting point, medium was removed and cells were incubated for 10 min with 3 mL of freshly prepared 10% formaldehyde at room temperature (RT). After the formaldehyde was removed, cells were washed with 60% isopropanol and incubated with 1 mL of Oil red O solution (Sigma) at RT for 10 min. The lipid droplet accumulation was analyzed under the microscope (Axiovert, Zeiss) and documented using the AxioVision software (Zeiss). The Oil Red O assay was performed in duplicates in three independent experiments.

## 2.4. RNA isolation, quantitative real-time PCR (qPCR), and gene expression profiling

Total RNA was extracted from cells using the RNeasy Mini kit (Qiagen) according to the manufacturer's protocol. Synthesis of cDNA, required for qPCR, was performed by using the First Strand cDNA Synthesis Kit (ThermoScientific) and following the manufacturer's protocol. Total RNA (1  $\mu$ g per sample) was reverse transcribed using the oligo(dT)18 primer included in the kit. For gene expression profiling 500 ng of total RNA per sample was amplified using the Illumina TotalPrep RNA Amplification kit (Ambion).

Quantitative real-time PCR was performed in triplicates in two independent experiments in 384-well plates (ThermoScientific) on a TaqMan 7900HT cyclor equipped with the SDS2.3 software (Applied Biosystems). Primers for the amplification and quantification of *Pparg* were previously described [30]. All other primers were newly designed by using the software Primer3 ([http://biotoools.umassmed.edu/bioapps/primer3\\_www.cgi](http://biotoools.umassmed.edu/bioapps/primer3_www.cgi)) [31]. Primers were synthesized by Metabion and are listed in Table 1.

The amplification was performed as follows: denaturation at  $95^\circ\text{C}$  for 10 min, 39 amplification and quantification cycles with  $95^\circ\text{C}$  for 15 sec and  $60^\circ\text{C}$  for 1 min, and finally a melting curve

**Table 1**  
Primers for qPCR.

Mouse gene	Name/Direction	Sequence (5'→3')	T <sub>m</sub> (°C)
<b>AUH</b>	mAUH_215_for	GGTGCTCGGGATTAACAGAG	60
	mAUH_423_rev	TGAGACAAAGGGACCAACT	58
<b>C/EBP<math>\beta</math></b>	mC/EBP $\beta$ _762_for	GACAAGCTGAGCGACGAGTA	60
	mC/EBP $\beta$ _919_rev	AGCTGCTCCACCTTCTCTG	60
<b>C/EBP<math>\alpha</math></b>	mC/EBP $\alpha$ _962_for	TGGACAAGAACAGCAACGAGTA	60
	mC/EBP $\alpha$ _1082_rev	GTCACCTCCAGCACCTTCTGT	61
<b>ELOVL3</b>	mELOVL3_133_for	CCCTACCCCAAGCTCTGTAA	60
	mELOVL3_349_rev	CGCGTTCTCATGTAGGTCTG	60
<b>HMGCR</b>	mHMGCR_426_for	GGTATTGCTGGCCTCTCAC	60
	mHMGCR_562_rev	CTCGCTCTAGAAAGGTCAATCA	60
<b>IPO8</b>	mIPO8_2267_for	CAGCAGGATTGCTTCGAGTA	58
	mIPO8_2434_rev	AGCATAGCACTCGGCATCTT	58
<b>MCEE</b>	mMCEE_457_for	CATCCACTGGGGAGTGATAGT	61
	mMCEE_648_rev	GGGATGGAGGAAAATCACAG	58
<b>MUT</b>	mMUT_377_for	ATTCACACGGGGACCATATC	58
	mMUT_570_rev	CAGCAACTCTGGGGTTGTCT	60
<b>MVD</b>	mMVD_37_for	GGGACTCCAGCATCTCAGTTA	61
	mMVD_253_rev	ATGCGGTCTCTGTGAAGTC	60
<b>PPAR<math>\gamma</math></b>	mPPAR $\gamma$ _for	TTTCAAGGGTGCCAGTTT	53
	mPPAR $\gamma$ _rev	AATCCTTGGCCCTCTGAGAT	58

program (95 °C for 15 sec, followed by 60–95 °C with a heating rate of 0.1 °C/sec). Signals were detected by fluorescence. The cycle threshold (CT) value was determined by the SDS2.3 software as the cycle at which the fluorescence rose markedly above the background fluorescence.

Relative gene expression was calculated using the comparative  $2^{-\Delta\Delta CT}$  method [32] and data were normalized to the house-keeping gene importin 8 (Ipo8; in pre-experiments tested to be suited) and the gene expression of samples at day 0 of adipogenic cell differentiation.

Gene expression profiling was conducted as previously described [33,34] using Illumina Mouse Ref-8 v2.0 Expression BeadChips and 500 ng cDNA per sample. Samples from 8 time points (days 0, 2, 4, 6, 8, 10, 14, and 18) were analyzed in three biological triplicates (except time point day 4 in duplicate). Data normalization (quantile algorithm) and background corrections were performed with the Illumina GenomeStudio 2011.1 software. Significant Analysis of Microarrays (SAM) was applied [35–37] to identify differential gene expression at seven time points (days 2, 4, 6, 8, 10, 14, and 18) compared to day 0 ( $n = 23$ ). Two to three biological repetitions per time point were assigned to separate groups and genes were considered as differentially regulated when the statistical analysis indicated a significant regulation in at least two of seven time points (fold change >1.8, FDR <10%). Cluster analysis was performed using self organizing tree algorithm (SOTA) [38] to identify groups of genes with similar expression patterns across the time course (growth termination criteria = 5 cycles). As distance function the Pearson correlation coefficient and the average distance were chosen. Expression data were submitted to the public repository database GEO [39] (identifier: GSE34150).

### 2.5. Western blotting

Cells collected in lysis buffer were lysed by three freeze–thaw cycles, and proteins were denatured by incubation with 4x Laemmli buffer at 95 °C for 10 min. After separation by PAGE, proteins were blotted onto a PVDF membrane using a semi-dry blotting apparatus of Bio-Rad. The proteins of interest were detected using primary antibodies against  $\beta$ -Actin, Ppar $\gamma$ , C/ebp $\beta$  and C/ebp $\alpha$  from Santa Cruz and appropriate secondary HRP-conjugated antibodies (Dianova and Sigma–Aldrich). After ECL detection (Pierce reagent), the images were captured using a Fusion FX7 apparatus (Vilber Lourmat).

### 2.6. Metabolomics measurement

At the day of experiment, cell suspensions were transferred to Precellys-Glass/Ceramic SK38 tubes (Peqlab) and homogenized in a Precellys24 apparatus (Peqlab) for 20 s at 5500 rpm. After centrifugation at  $18.000 \times g$ , 20  $\mu$ L of the supernatant was used for metabolomics measurements. Conditioned media were directly applied to kits without any pre-treatment.

Metabolite concentrations were determined in the cells (extracts) and conditioned media. Three different targeted metabolomics assays from Biocrates Life Sciences AG (Innsbruck, Austria) were applied. The AbsoluteIDQ p180 kit assay was used to quantify up to 188 molecules including amino acids (AAs), phosphatidylcholines (PCs), lysoPCs, sphingomyelins (SM), carnitines (Cs), and hexoses (H); this assay was performed in the Helmholtz Zentrum München as described previously [40,41]. Two assays for fatty acid and prostaglandin quantification were performed directly at Biocrates as previously described [42]. The samples for the AbsoluteIDQ p180 kit analyses were prepared in triplicates in three independent experiments. Fatty acids and prostaglandin quantification was performed out of the samples prepared in three

independent experiments.

The statistical data analysis was performed with the *metaP* server at the Helmholtz Zentrum München (<http://metabolomics.helmholtz-muenchen.de/metap2/>), which provided automated and standardized data analysis for metabolomics data [43]. Self-organising tree algorithm (SOTA) cluster analysis [38] was applied on the fold changes of metabolite concentrations relative to day 0 to identify groups of metabolites with similar patterns across the time course (growth termination criteria = 5 cycles). As distance function the Pearson correlation coefficient and average distance were chosen.

Functional data analysis was performed with Ingenuity Pathway Analysis (IPA; Qiagen; <http://www.ingenuity.com/products/ipa>) as well as Kyoto Encyclopedia of Genes and Genomes (KEGG; <http://www.genome.jp/kegg/>).

## 3. Results

### 3.1. Metabolomics combined with transcriptomics: a comprehensive tool to study adipogenesis

In order to monitor changes occurring at different stages of adipogenesis, we differentiated 3T3-L1 cells for 18 days and collected samples at the 8 time points, namely at day 0, 2, 4, 6, 8, 10, 14, and 18 (the experimental design is presented in Fig. 1A). Differentiation of confluent preadipocytes was initiated by growth medium containing insulin, dexamethasone and IBMX and after day 4 the cells were matured in medium supplemented with only insulin as described [44]. The accumulation of lipid droplets and the analysis of the transcription factors C/ebp $\beta$ , Ppar $\gamma$ , and C/ebp $\alpha$  essential for the regulation of lipid homeostasis [45] on the mRNA and protein levels demonstrated ongoing adipogenesis (results presented in Fig. 1B, C, and D). The two bands observed on the western blot of PPAR $\gamma$  may reflect two isoforms of this protein, which were reported as specific to adipose tissue [46].

Next, metabolomics analyses were performed on both the cells and corresponding conditioned media. Out of the 188 molecules detected by the AbsoluteIDQ p180 kit, 115 metabolites from different metabolic classes (amino acids, carnitines, biogenic amines, hexoses and phospholipids) were quantified and used for further analysis. In the first place we verified whether metabolic alterations have biological background (are correlating with time course) or technical background (are correlating with sample preparation) by using Kendall correlation test. As shown in Suppl. Fig. 2 metabolic alterations were dependent on the adipogenic cell differentiation but not caused by the sample preparation procedure.

In order to reveal a structure in our metabolic data we applied the principal component analysis (PCA) for both conditioned media and the cells. The PCA plots clearly demonstrated the differences between examined days of adipogenesis (Fig. 2A). Furthermore, PC1 and PC3 strongly reflected the time course of adipogenesis from undifferentiated cells through adipogenic differentiation to mature adipocytes. A tight clustering of biological replicates in both conditioned media and cells indicates high similarity among the samples from the same time point. We further applied a bidirectional cluster analysis on the fold changes (in relation to pre-adipocytes (day 0)) of cellular metabolite concentrations to identify clusters of metabolites. The heatmap presented in Fig. 2B shows on the one hand clusters of sample replicates, reflecting the same patterns as were seen in the PCA plots (days of cell differentiation/maturation), and on the other hand six clusters of metabolites. Metabolites grouped in cluster I and II showed down-regulation in the differentiation phase (days 2–6) and up-regulation in the maturation phase. In this cluster we found the majority of

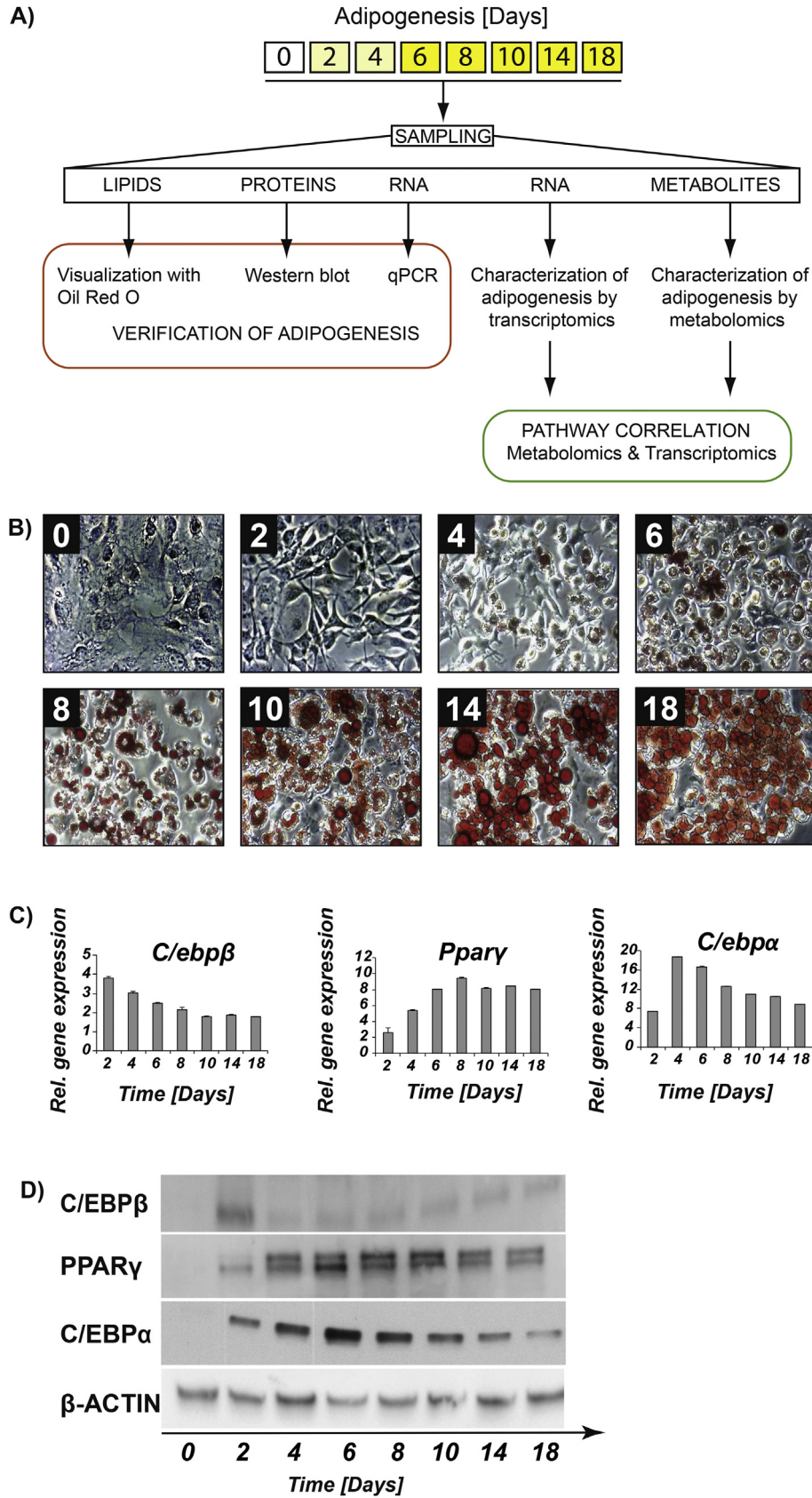


**Fig. 1.** Overview of experimental design and monitoring of adipogenesis A) Overview of the study design. Murine 3T3-L1 cells were differentiated from preadipocytes to adipocytes over 18 days. Cell and corresponding medium samples of 8 different time points (see squares) were collected and examined as indicated in the workflow. The intensity of yellow colour in the squares corresponds to the progression of adipogenesis. White – non-differentiated cells; light yellow – differentiation phase; dark yellow – maturation phase. Cell differentiation was verified by monitoring the lipid droplet accumulation with Oil red O assay (B) and the photos were taken at 200-fold magnifications. C) The expression patterns of transcription factors *Pparγ*, *C/ebpβ* and *C/ebpα*, known to promote adipogenesis, were evaluated with quantitative PCR. D) Western blot analyses of *PPARγ*, *C/EBPα* and *C/EBPβ*. The two bands observed for *PPARγ* reflects its two isoforms. The first band from top reflects *PPARγ2* and the second one the *PPARγ1*.

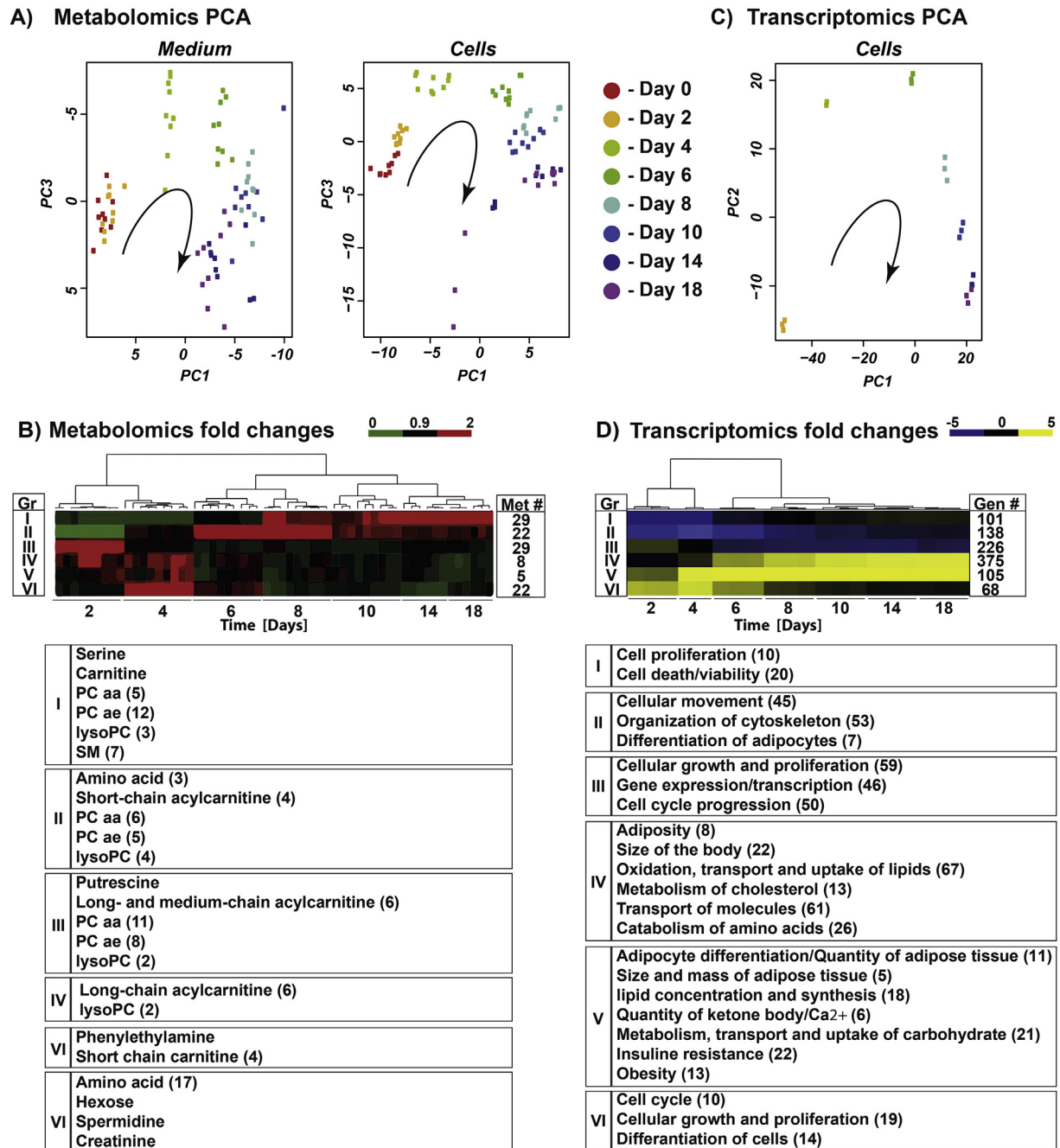


**Fig. 2.** Combined metabolomics and transcriptomics enable a broad analysis of adipogenesis. We have analysed the transcriptome and the metabolome during adipogenesis in cells. Metabolite measurements were performed with the AbsoluteIDQ p180 kit assay and the transcriptomic analysis using the Illumina BeadChip technology. PCA plots of metabolomics data (A) is based on 115 metabolites in the medium and in cells. The PCA plot of transcriptomics data (C) is based on top 1012 regulated genes. Colour code for days of adipogenesis: red – day 0, orange – day 2, light green – day 4, dark green day 6, light blue – day 8, blue – day 10, dark blue – day 14 and violet – day 18. Arrows in (A) and (C) depict the progression of adipogenesis. B) Results of SOTA cluster analysis of the 115 metabolites in cells with the overview on metabolite classes in each group. The fold changes are shown on a 0.0 (down-regulation, green) to 2 (up-regulation, red) scale. Gr – group (cluster) number, Met# – number of metabolites in the group. D) Gene expression profiling at indicated days of adipogenesis. SOTA cluster analysis of the top 1012 regulated genes with the functional assignment of the groups (I–VI) using IPA. Gen# – number of genes in the group. The fold changes are shown on a –5.0 (down-regulation, blue) to 5 (up-regulation, yellow) scale. Table in (B) shows the metabolite class together with number of metabolites in each class and table in (D) shows the gene category/function together with the amount of genes classified.

phospholipids, and short chain carnitines, carnitine, as well as three amino acids namely asparagine, aspartic acid, and glutamine. Metabolites assigned to cluster III – VI were up-regulated during the differentiation phase (days 2–6) and displayed down- or no regulation in the maturation phase. In the cluster III phosphatidylcholines and long- as well as medium-chain acylcarnitines were grouped, whereas in cluster VI mainly amino acids were found.

In parallel to metabolomics, we performed transcriptomics by using the Affimetrix Bead technology on cell samples from the 8 time points. The statistical data analysis was performed with the fold changes of gene expression in relation to data for pre-adipocytes at day 0. We identified 1012 genes significantly regulated in at least 2 of 7 time points (Suppl. Fig. 3). As in case of metabolomics, we applied PCA to reveal a structure in the

transcriptomics data. The PCA analysis of 1012 significantly regulated genes (Fig. 2C) resulted in a pattern similar to that visible in the PCA plot of the cell metabolomics data (Fig. 2A). The PCA of the transcriptomics data was exhibiting clear differences between the days of differentiation and maturation, with simultaneous tight clustering of the replicates. A bidirectional cluster analysis of the regulated genes confirmed the tight clustering of the biological replicates of each time point and enabled grouping of regulated genes into six clusters containing 68 to 375 genes per group (Fig. 2D). Genes in clusters II and V showed uniform up- (cluster V) or down-regulation (cluster II) during the whole period of adipogenesis. Genes of clusters III and IV displayed no changes of expression levels during the first 4 days, but were strongly regulated at later time points. Expression of the genes of clusters I and VI were changed during the first 6 days but were not regulated in comparison to day 0 between days 6–8.

The assigned groups of genes were characterized by functional annotations (Fig. 2D). Genes organized in the clusters I–III and VI reflect early molecular events, essential for reprogramming of the cell fate, i.e., the change from the fibroblast-like to the fat-accumulating adipocyte. For instance in cluster two, well known signatures of loss of pre-adipocyte-like phenotype namely changes in  $\beta$ - and  $\gamma$ -actin and  $\alpha$ - and  $\beta$ -tubulin [47] were found. Furthermore, genes organized in cluster III and belonging to the category ‘cellular growth and proliferation’ were associated with growth arrest, occurring at early stages of adipogenesis [48]. Genes annotated with ‘differentiation of adipocytes, obesity, and adiposity’ were highly represented in the clusters II, IV and V. In particular, known attributes of the phenotype of fat cells were found in those groups, like for example the cell death-inducing DFFA-like effector (CIDEC), adipogenin, adiponectin, PPAR $\gamma$  and stearoyl-CoA 9-desaturase (SCD). Because our main objective was to study metabolic processes occurring during adipogenesis and in mature adipocytes we were interested in genes assigned to the following functional groups: ‘oxidation, transport, and uptake of lipids’, ‘metabolism of cholesterol’, ‘quantity of ketone body/Ca<sup>2+</sup>/steroid’ and ‘metabolism, transport, and uptake of carbohydrate’, to complement the metabolic data. By using the IPA software for the analysis of combined metabolomics and transcriptomics data, we were able to elucidate direct links between regulated genes and regulated metabolites as is outlined in the following chapters.

Thus, metabolomics data can complement gene expression data and *vice versa*, making pathway analysis more efficient and comprehensive.

### 3.2. Branched chain amino acid metabolism is strongly regulated during adipogenesis

We were particularly interested in the BCAA metabolism, because previous reports showed discrepancies between the behaviour of those molecules in children/adolescents [14,15] and adult human individuals [13] suffering from obesity, which could be related to the dynamics of fat cell turnover [16]. We reasoned that identification of metabolic pathways connected to the BCAA metabolism could let us understand previously observed differences as well as reveal therapeutic targets or biomarkers enabling obesity prediction.

In our study BCAAs were significantly down-regulated in both conditioned media and cells (Fig. 3A and B). Thus, in the first place we were screening our data set of 1012 significantly regulated genes for those genes associated with the BCAA metabolism. Fig. 3C presents the reconstructed pathway based on metabolomics and gene expression data.

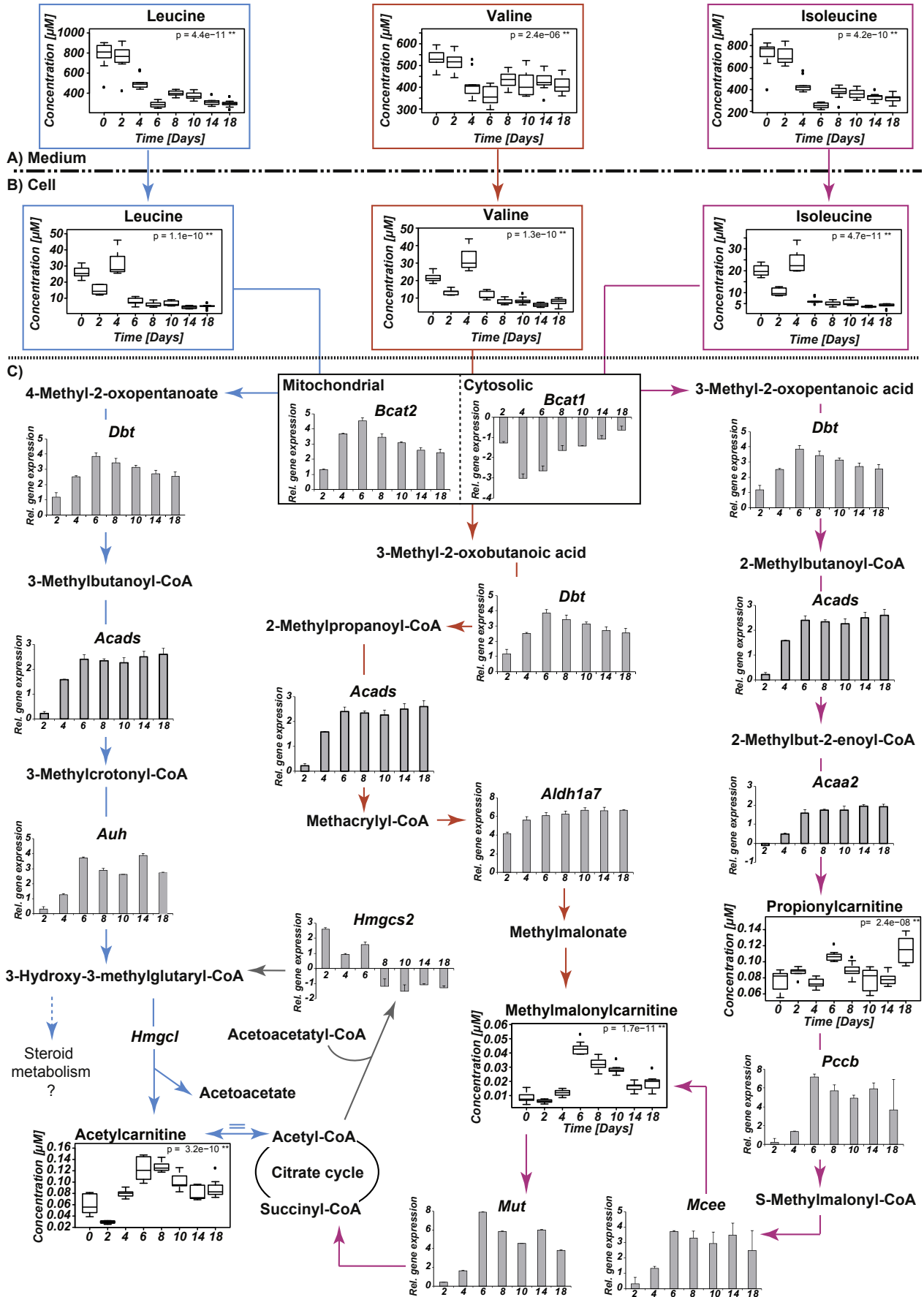
The cells entering the differentiation phase (day 2) exhibited a

significant decrease in all BCAA levels (Fig. 3A and B). However, at day 4 an increase of intracellular and significant decrease of extracellular BCAA levels was observed. The maturation phase (starting at day 6) was characterized by a BCAA decrease in both cells and conditioned medium.

Our results on the metabolite level in cells agreed with the gene expression profiling showing an up-regulation of genes of the BCAA catabolic pathway (Fig. 3C). The up-regulation of the mitochondrial branched chain amino-acid transaminase 2 (*Bcat2*) and down-regulation of the cytosolic *Bcat1* suggested a preferred BCAA-degradation in mitochondria of mature adipocytes. The expression of genes involved in BCAA catabolism reached their maximum exactly at day 6 when all of the BCAAs were significantly down-regulated. Because we used a targeted metabolomics approach, the number of measured metabolites was limited. For instance, 3-hydroxy-3-methylglutaryl-CoA (leucine catabolism), methylmalonate (valine catabolism) and methylmalonyl-CoA (isoleucine breakdown), which are products of the BCAA catabolism, were not measured with our assay. However, genes involved in their synthesis (*Auh*, *Aldh1a7*, and *Pccb*) were strongly up-regulated, which suggests an up-regulation of synthesis of those molecules in the system. We further examined the possible connection of the BCAA degradation pathway to other metabolic pathways. Hypothetically, all the above mentioned BCAA breakdown products can be incorporated into the tricarboxylic acid (TCA) cycle. However, the 3-hydroxymethyl-3-methylglutaryl-CoA lyase (*Hmgcl*), involved in the conversion of 3-hydroxy-3-methylglutaryl-CoA into acetoacetate and acetyl-CoA, has not been found among the 1012 significantly regulated genes, which suggest incorporation of 3-hydroxy-3-methylglutaryl-CoA into the steroid metabolism (as speculated in Fig. 3C). In conclusion, BCAAs catabolism is strongly up-regulated during adipogenesis and in mature adipocytes, suggesting their significant role in fat cell metabolism.

### 3.3. Leucine degradation products are linked to cholesterol biosynthesis

Based on the above data, we investigated the (possible) connection between the BCAA degradation pathways and other metabolic events occurring during adipogenesis and in mature adipocytes. As shown in Fig. 3C, leucine can be degraded to 3-hydroxy-3-methylglutaryl-CoA, which is one of the intermediates of the cholesterol synthesis pathway. The 3-hydroxy-3-methylglutaryl-CoA synthase (*Hmgcs2*), involved in production of cholesterol-convertible 3-hydroxy-3-methylglutaryl-CoA [49], and 3-hydroxy-3-methylglutaryl-CoA reductase (*Hmgcr*), involved in mevalonate synthesis, are two sequential enzymes in the cholesterol biosynthetic pathway [50]. Interestingly, *Hmgcs2* was up-regulated only from day 0 to day 6 of adipogenesis and down-regulated afterwards (Fig. 3A), whereas *Hmgcr* was up-regulated from day 6 until day 18. Simultaneously, the AU RNA binding protein/enoyl-CoA hydratase (*Auh*; also known as methylglutaconyl-CoA hydratase) that is a part of the leucine catabolic pathway and catalyzes the synthesis of 3-hydroxy-3-methylglutaryl-CoA, which may serve as product for cholesterol synthesis, was up-regulated starting from day 6 (Fig. 4A). These results indicate a metabolic switch at day 6 (the beginning of the maturation process) in the cholesterol synthesis pathway, which starts to be supplied by the leucine degradation product. As shown in Fig. 4B, 3-hydroxy-3-methylglutaryl-CoA can be incorporated into the cholesterol synthesis pathway through mevalonate, trans-trans-farnesyl diphosphate, dimethylzosterol, zymosterone and lathosterol. The respective genes involved in the transformation of 3-hydroxy-3-methylglutaryl-CoA into cholesterol were strongly up-regulated (see Fig. 4B). The presented results showed a possible



link between leucine degradation and the cholesterol synthesis pathway.

### 3.4. Interlink between isoleucine degradation and odd chain fatty acid synthesis

We further investigated the catabolic pathway of the two other BCAAs valine and isoleucine. The isoleucine/valine degradation pathway is connected to the citrate cycle (see Fig. 3C), which can supply fatty acid synthesis or/and elongation through the acetyl-CoA molecule. Thus, we analysed changes in the fatty acids composition of cells during adipogenesis. Those fatty acids, which were altered during adipogenesis, are presented in Fig. 5. Surprisingly, among the regulated molecules we found only three even chain fatty acids with saturated (Fig. 5A) and unsaturated (Fig. 5B) chains. The majority were odd chain fatty acids with saturated (Fig. 5C) and unsaturated chains (Fig. 5D), which were previously described as not synthesized by mammals as well as biomarkers of dairy product consumption [51]. Because we used the cell growth medium supplemented with 10% fetal bovine serum and the ruminant animals contain approximately 5% of odd chain fatty acids in their tissue [52], the increased odd chain fatty acid content in cells may have arisen from the culture medium. Consequently, free odd chain fatty acid concentrations in the conditioned medium were investigated. As shown in Fig. 5E the odd chain fatty acids were up-regulated also in the medium. Thus, odd chain fatty acids seemed to have been net produced by adipocytes and not only taken up from the conditioned medium. There are two possible pathways for odd chain fatty acid synthesis: either the even number fatty acids can undergo alpha-oxidation or alternatively can be *de novo* synthesised from propionyl-CoA as starting molecule [53]. The genes involved in alpha-oxidation of fatty acids have not been detected in our 1012 significantly regulated genes, therefore we further explored the alternative pathway, namely the synthesis of odd chain fatty acids from the propionyl-CoA molecule. Because isoleucine is catabolized to propionyl-CoA, we suggested a crosslink between isoleucine degradation and odd chain fatty acid synthesis. Indeed, we found propionyl-carnitine (the transport form of propionic acid) in our metabolite panel to be slightly up-regulated (Fig. 6B), which could be seen as a hint that the isoleucine degradation product propionyl-CoA can possibly be used for *de novo* synthesis of odd-chain fatty acids. Besides, we observed an up-regulation of acetyl-carnitine (transport form of acetic acid) during adipogenesis (Fig. 6A), which supports the suggestion that valine and isoleucine catabolism may support fatty acid elongation or *de novo* fatty acid synthesis by supplying acetyl-CoA (as shown in Fig. 3C). The alteration patterns of e.g. tridecanoic (C13:0) or myristic acids (C14:0) reached their highest peak during the adipocyte differentiation process, followed by a decrease in the maturation phase (Fig. 5A and B). The decrease during maturation might indicate that these molecules are intermediates for elongation processes. Indeed, fatty acids with longer chain length remained up-regulated also during the maturation phase (Fig. 5A and B). The alterations in fatty acid metabolism correlated with the expression of genes involved in fatty acid elongation (*Elovl3*) (Fig. 6C) and desaturation (*Fads2* and *Scd1*) (Fig. 6D). The role of *Elovl3* in

elongation of saturated and monounsaturated fatty acid chains containing between 16 and 24 carbons was previously reviewed [54]. Among the genes involved in fatty acid elongation, only *Elovl3* was detected in our gene expression data set. Among the genes identified in our data set which were involved in fatty acid desaturation (*Fads1*, *Fads2*, *Fads3*, and *Scd1*), only *Fads2* and *Scd1* met the criteria of significant regulation (fold changes higher than 1.5 in relation to day 0). The possible patterns of fatty acid metabolism are presented in Fig. 6E and F. Since fatty acids can be further metabolized to glycerophospholipids (PCs), also these molecules were investigated. The correlation between adipogenesis progression and the accumulation of acyl–acyl (aa) phosphatidylcholines (PCs) and acyl-ether (ae) PCs with an increased saturation number and carbon chain length was observed. The unique, previously not reported patterns of phosphatidylcholines suggested that during adipogenesis unsaturated fatty acids are incorporated preferentially into the aa PCs (Fig. 7A and C) and elongated fatty acids into the ae PCs (Fig. 7B and D). Collectively, our data show a strong regulation of the fatty acid and the glycerophospholipid metabolism and suggest a link between odd chain fatty acid synthesis and isoleucine degradation, because isoleucine is a possible main supplier of primer molecules for this pathway.

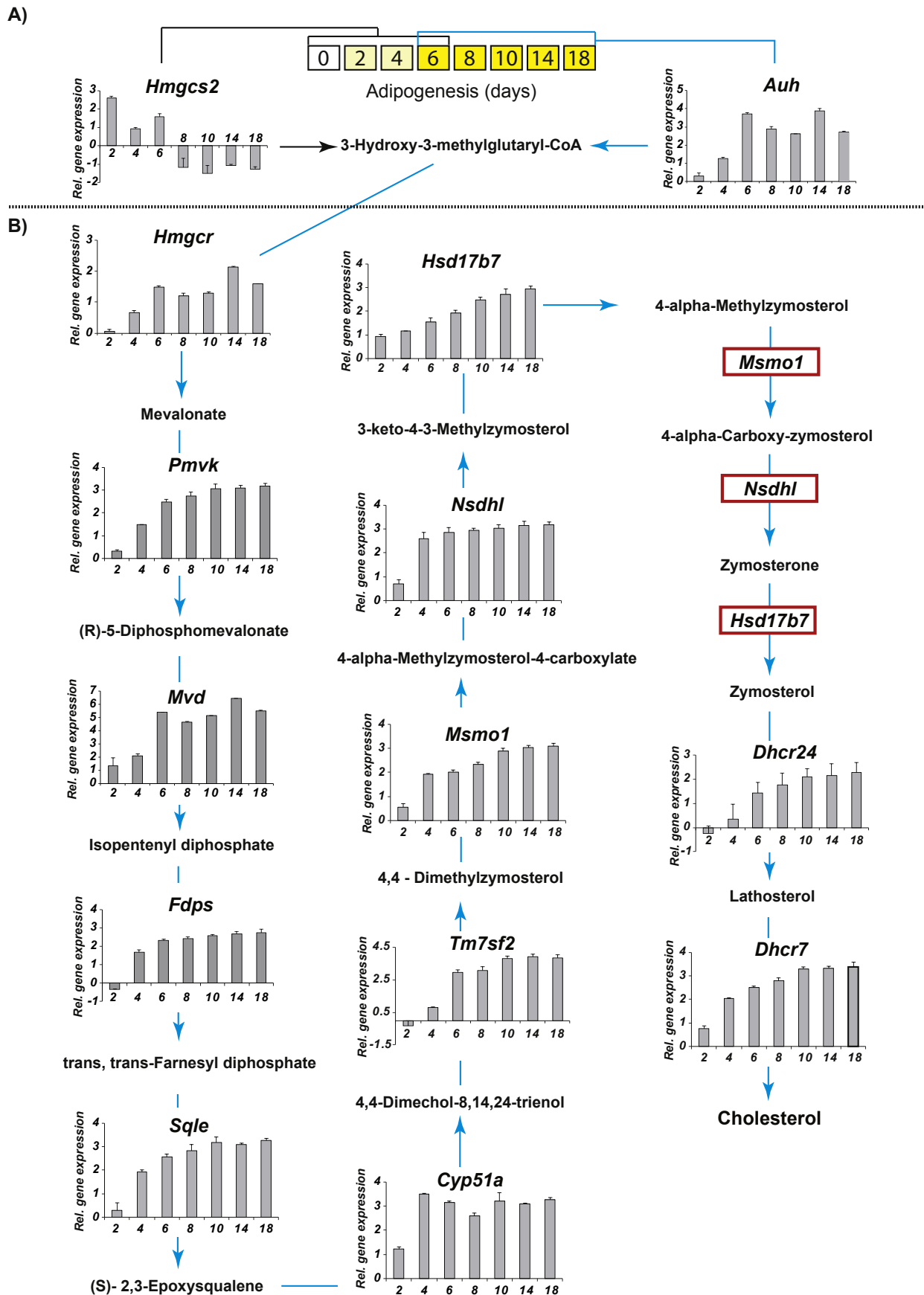
## 4. Discussion

Obesity is a highly complex disorder as it arises from the interaction of multiple genes with environmental and behavioural factors, making its prevention and management particularly challenging [55]. Recently, the newly emerging deep-phenotyping technology called metabolomics, which is based on the metabolic profiling of human individuals in large population studies, has enabled the prediction of metabolic diseases before they become clinically evident [56–59]. In addition, the determination of molecules predictive for the development of this complex disease may change current treatment strategies.

Metabolic studies on human obesity have been performed in both obese children [14,15] and adults [13]. However, the reported behaviour of molecules distinguishing the investigated groups (healthy lean children vs obese children and children with type 2 diabetes or healthy lean adults vs obese adults) were not consistent. Increased BCAA levels in obese adults [13] and decreased BCAA levels in obese children and adolescents [14,15] were reported as signatures of obesity. Recently, the dynamics of fat cell turnover during human life was revealed by Spalding et al. [16]. The major factor determining fat mass in human adults is adipocyte number. However the quantity of fat cells remains constant in adults [16] and this amount is established during childhood and adolescence. Thus, differences in BCAA patterns between children/adolescents and adults could be associated with diverse fat cell metabolism during the life span of individual. Therefore, the investigation of the BCAA metabolism and its link to other pathways, especially during adipogenesis and in mature adipocytes, may provide additional information, which could reveal potential biomarkers predicting obesity and/or novel drug targets.

Here, we combined for the first time metabolomics and transcriptomics to study adipogenesis in an established cell culture

**Fig. 3.** Catabolic pathway of BCAAs is regulated during adipogenesis. We have compiled measured data from metabolome and transcriptome analyses for cell samples of 8 different time points (days 0, 2, 4, 6, 8, 10, 14, and 18 of adipogenesis). Metabolite concentrations are shown as boxplots and changes in gene expression levels as bar graphs. Alteration patterns of BCAAs are shown for conditioned media (A) and cells (B). C) Schematic illustration of BCAA catabolism data including expression data (Illumina Bead Chip data) of indicated genes and concentration data of metabolites (AbsoluteIDQ) along the pathways. Leucine degradation pathway is indicated with blue, valine catabolism with orange and isoleucine breakdown with pink arrows and lines. Grey arrows indicates a metabolic pathway which is not a direct part of BCAA breakdown. Genes involved in BCAA catabolism are highlighted by bold italic font and metabolites by bold font. Metabolites not determined in this study but added for pathway integrity are indicated by bold font without boxplot diagram.



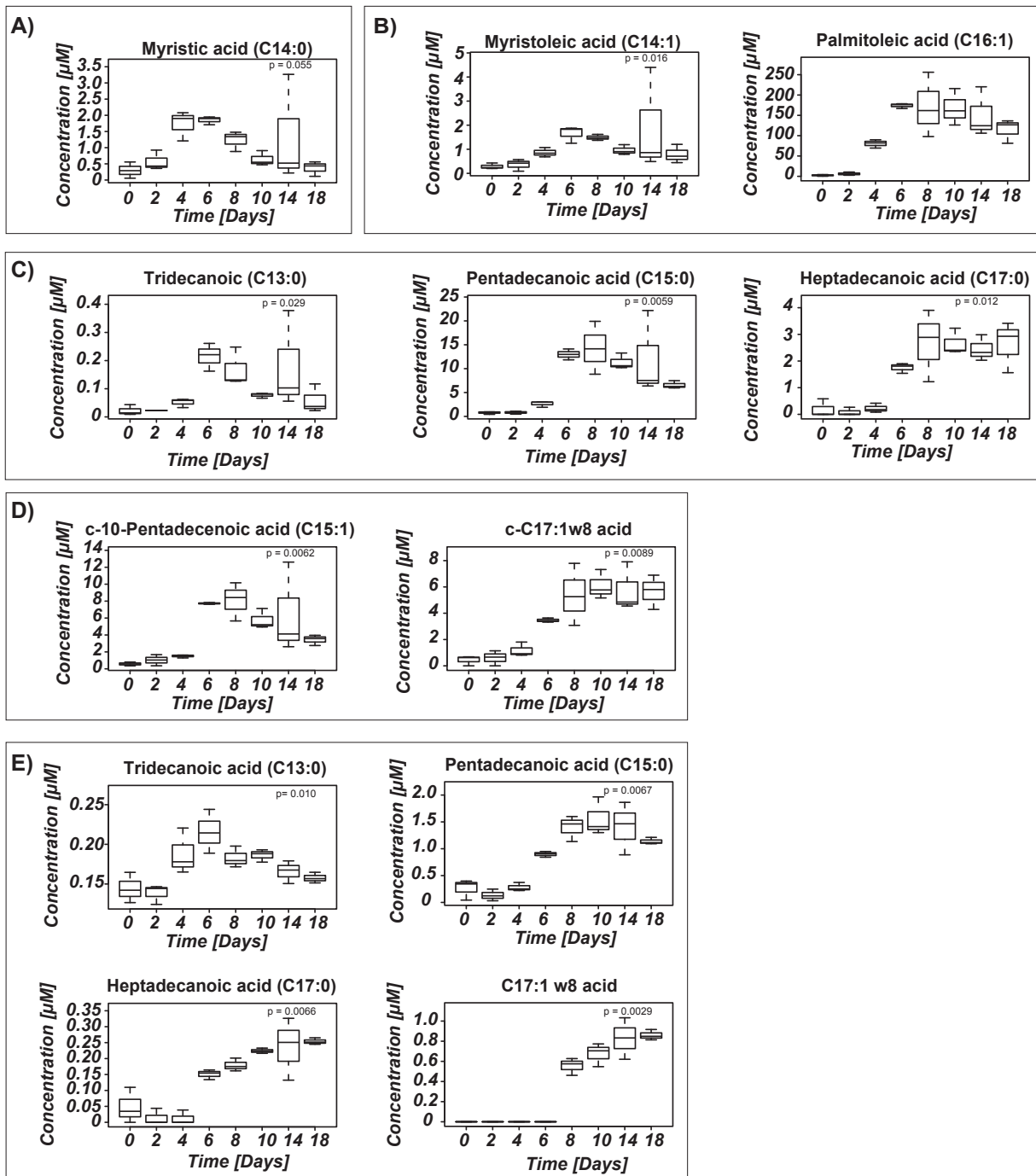


**Fig. 5.** Fatty acids chain composition changes during adipogenesis A-D) Fatty acids that significantly changed their concentration during adipogenesis are shown; saturated (A) and unsaturated (B) even-chain fatty acids are depicted as well as saturated (C) and unsaturated (D) odd-chain fatty acids. E) Changes in free fatty acid levels in the conditioned medium. The characteristics of the fatty acid chains is indicated as Cx:y, where x represents the carbon chain length and y the number of double bonds.

model. This experimental design offers a broader view on the metabolism and crosstalk between the metabolic pathways during differentiation and in mature adipocytes. Cells were harvested by scraping instead of by trypsinization, as recently applied in the metabolic phenotyping of adipogenesis [26], to avoid cell membrane damage [60] and metabolite leakage. We have undertaken precautions to ensure validity of collected samples. The tight clustering of replicates on the PCA plots of both metabolomics and transcriptomics data is demonstrating high quality of our study.

We found significantly regulated metabolites correlating with

differentially expressed genes, which exhibited characteristic patterns for different stages of adipogenesis. Our studies are in good agreement with previous reports on transcriptomics [20–22] and metabolomics [26] of adipogenesis. Furthermore, metabolic alteration of the polyamines putrescine and spermidine (Fig. 1B) are consistent with a recent study highlighting that these molecules are associated with lipid accumulation and adipogenesis [61]. In addition, the decreased palmitoylcarnitine (C16) concentration in the cells (data not shown) is in agreement with a previous study that reported a reduction in carnitine concentrations (nonesterified

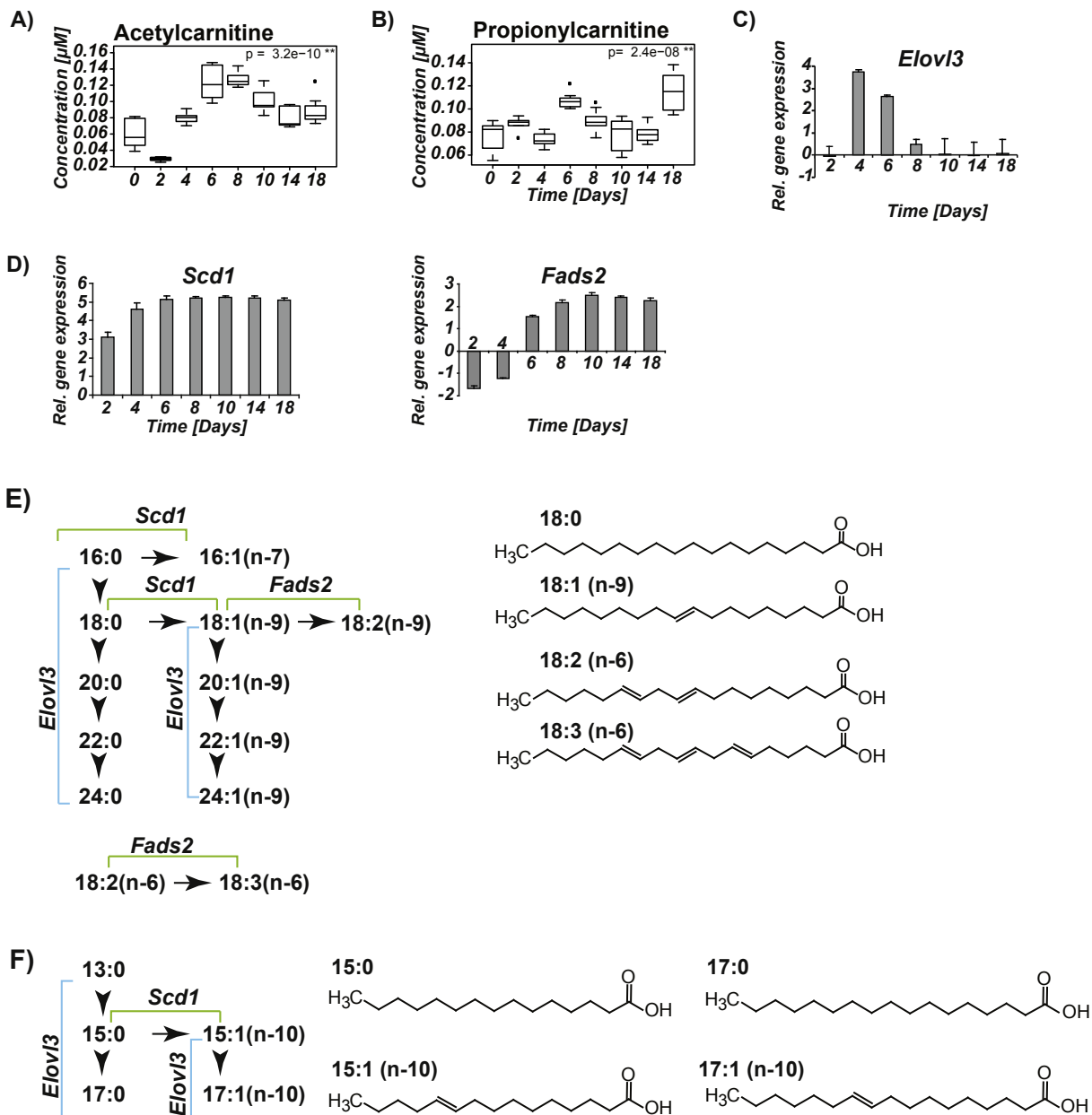


**Fig. 6.** Valine and isoleucine degradation products are linked to the even- and odd-chain fatty acid synthesis during adipogenesis. A) acetylcarnitine and B) propionylcarnitine concentrations might reflect the propionyl-CoA and acetyl-CoA pool during adipogenesis. C) Gene expression patterns of elongase *Elov13* and (D) desaturases *Scd1* and *Fads2* at corresponding days of adipogenesis. Schematic illustration of possible saturation and elongation steps for even (E) and odd (F) chains fatty acids. Selected fatty acids are shown as well. The characteristics of fatty acid chains is indicated as x:y or x:y(n-z), where x represents the carbon chain length, y the number of double bonds, and n-z the positions of the double bonds.

carnitine, acid-soluble acylcarnitines, and acid-insoluble acylcarnitines) during adipogenesis [62]. However, previous studies on metabolic changes during adipogenesis did not reveal any regulation in the BCAA metabolism.

We also compared our results with studies on human individuals suffering from obesity, since we reasoned that fat cells have some significant impact on the overall composition of body fluids. We found that some metabolic alterations seen in our cell culture study, such as elevated levels of glutamine, asparagine, and fatty acids including myristic, myristoleic, and palmitoleic acid correspond to the results of a study in obese adult individuals [13]. In contrast, our results regarding BCAA metabolism are not consistent with reports describing an increase in BCAAs as a signature for obese adults. However, the biofluids of children

suffering from obesity and type 2 diabetes were characterized by a significant decrease in BCAA concentrations, similar to our current results. Decrease in BCAAs level during adipogenesis, observed in our study, together with previous Spalding's report [16], may explain the discrepancy in the study on BCAA metabolism between children/adolescents and adults. It could be concluded that increased BCAA levels can be considered as a signature of obese individuals, while a decrease might point to the formation of new fat cells a process which is limited to occur only in children and adolescents [16]. Therefore, decreases in BCAA level in children can be considered as a biomarker for obesity development.

In a further step, we investigated the involvement of BCAA catabolism products in the cellular metabolic network. We uncovered a novel link between branched chain amino acids and lipid

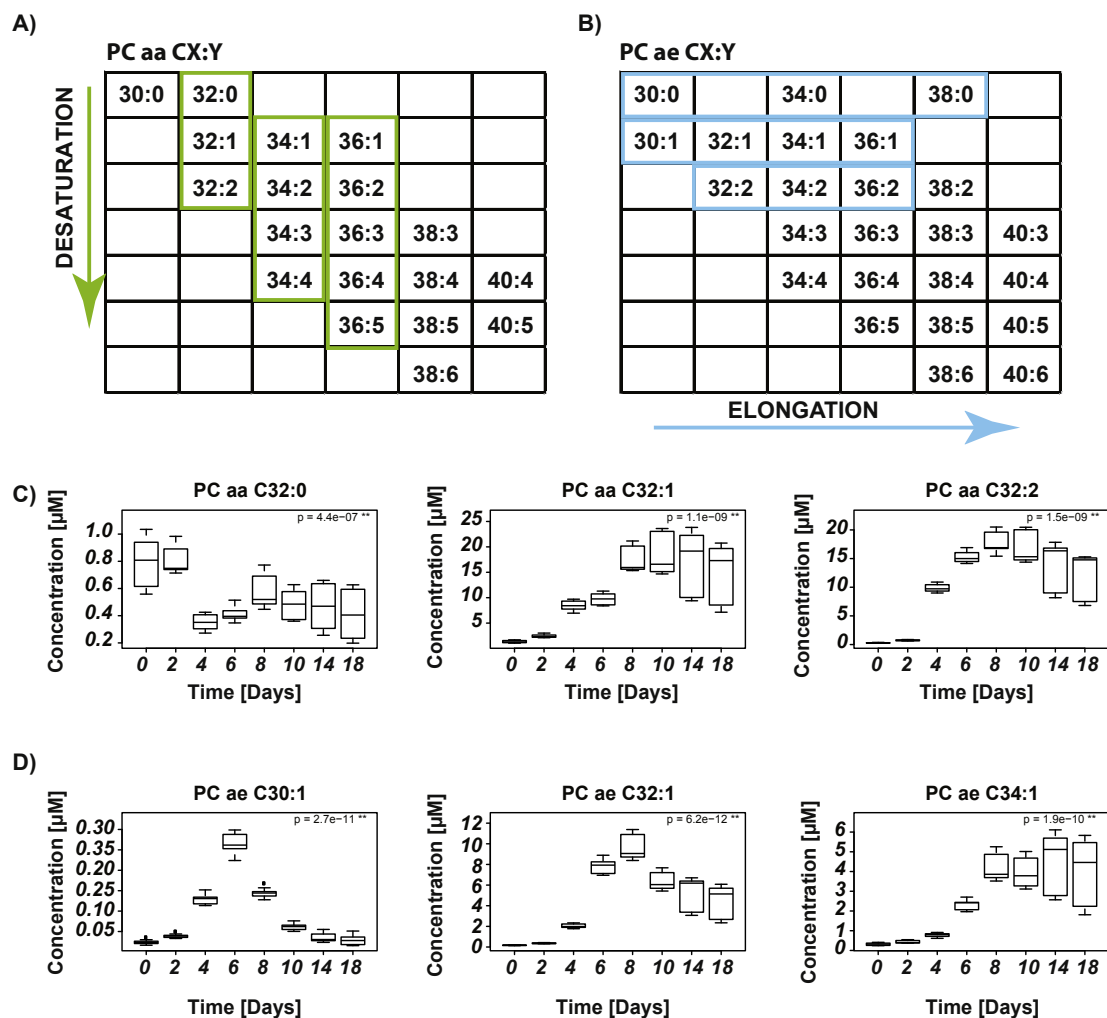


**Fig. 7.** Metabolic patterns of phosphatidylcholines at different stages of adipogenesis A-B) Schematic illustration showing significantly altered phosphatidylcholines (PCs) with acyl–acyl (aa) (A) and acyl–ether (ae) (B) chains. PCs highlighted by green frames reflect reactions of increasing desaturation and those marked by blue frames reflect reactions of increasing elongation observed in PCaa and PCae, respectively. C-D) Concentration patterns of selected PC aa and PC ae (D) metabolites in cells during adipogenesis are shown: (C) PC aa metabolites of left green box in (A) are displayed; PCaa with higher double-bond number are more abundant with ongoing adipogenesis. (B) PC ae metabolites of the middle blue box in (B) are displayed; molecules with longer fatty acid chains demonstrate increase in concentration during adipogenesis.

metabolic pathways during adipogenesis and in mature adipocytes. To date, leucine conversion into lipids and sterols was only hypothesized [63]. In this study, we noted that the leucine degradation product 3-hydroxy-3-methylglutaryl-CoA may serve as a substrate for cholesterol biosynthesis. Furthermore, we observed a connection between an increase in isoleucine degradation and the accumulation of odd chain fatty acids. During metabolic pathway analysis we found that propionyl-CoA, which is a product of isoleucine degradation, might be a substrate for odd chain fatty acid synthesis. Although previous studies have suggested that odd chain fatty acids cannot be metabolised in the human body and are delivered via the diet only [51], our study clearly demonstrated that odd chain fatty acids can be produced by adipocytes and accumulate during differentiation. Notably, an enhanced synthesis of odd-numbered long chain fatty acids stimulated by an excess of propionyl-CoA has been found in red cell membrane lipids of patients with propionic acidemia and methylmalonic aciduria, which are disorders of the propionate catabolism [64].

In conclusion, the altered patterns of BCAAs presented in the current study are consistent with metabolic data from obese children and adolescents, which may be related to the dynamics of fat cell turnover during human life [16]. We also revealed the potential

mechanism involved in the metabolic switch, which links BCAA catabolism with cholesterol synthesis. Therefore, the decreased BCAA concentrations should be further investigated toward their potential role as novel biomarkers determining human obesity development already in children. In this work, we presented a decrease in BCAAs, and accumulation of odd chain fatty acids, and phosphatidylcholines as biomarkers of adipogenesis, thereby suggesting a potential role as biomarkers for obesity prediction.

#### Acknowledgements

We thank Gabriele Zieglmeier (Helmholtz Zentrum München) for her excellent technical assistance in cell culture. We thank Julia Scarpa, Dr. Werner Römisch-Margl and Katharina Faschinger for support with the metabolomics measurements performed at the Helmholtz Zentrum München, Genome Analysis Center, Metabolomics Core Facility. Support for some of the experiments was provided by the Weill Cornell Medical College in Qatar bioinformatics and virtual metabolomics core, which is funded by the Qatar Foundation.

This study was supported in part by a grant from the German Federal Ministry of Education and Research (BMBF) to the German

Center Diabetes Research (DZD e.V.) and by the Helmholtz Alliance ICEMED (grant to JB). The funders had no role in study design, data collection and analysis, decision to publish, or preparation of the manuscript.

## Appendix A. Supplementary data

Supplementary data related to this article can be found at <http://dx.doi.org/10.1016/j.abb.2015.09.013>.

## References

- [1] C.J. Lavie, R.V. Milani, H.O. Ventura, Obesity and cardiovascular disease: risk factor, paradox, and impact of weight loss, *J. Am. Coll. Cardiol.* 53 (2009) 1925–1932.
- [2] J.S. Flier, Obesity wars: molecular progress confronts an expanding epidemic, *Cell* 116 (2004) 337–350.
- [3] A. Guilherme, J.V. Virbasius, V. Puri, M.P. Czech, Adipocyte dysfunctions linking obesity to insulin resistance and type 2 diabetes, *Nat. Rev. Mol. Cell Biol.* 9 (2008) 367–377.
- [4] E.E. Calle, M.J. Thun, Obesity and cancer, *Oncogene* 23 (2004) 6365–6378.
- [5] Y. Ma, Y. Yang, F. Wang, P. Zhang, C. Shi, et al., Obesity and risk of colorectal cancer: a systematic review of prospective studies, *PLoS One* 8 (2013) e53916.
- [6] J. Ligele, Obesity and breast cancer, *Oncol. Willist. Park* 25 (2011) 994–1000.
- [7] C.L. Amling, Relationship between obesity and prostate cancer, *Curr. Opin. Urol.* 15 (2005) 167–171.
- [8] E.E. Calle, M.J. Thun, J.M. Petrelli, C. Rodriguez, C.W. Heath Jr., Body-mass index and mortality in a prospective cohort of U.S. adults, *N. Engl. J. Med.* 341 (1999) 1097–1105.
- [9] A.J. Stunkard, T.I. Sorensen, C. Hanis, T.W. Teasdale, R. Chakraborty, et al., An adoption study of human obesity, *N. Engl. J. Med.* 314 (1986) 193–198.
- [10] J.R. Speakman, Obesity: the integrated roles of environment and genetics, *J. Nutr.* 134 (2004) 2090S–2105S.
- [11] K.J. Dick, C.P. Nelson, L. Tsaprouni, J.K. Sandling, D. Aissi, et al., DNA methylation and body-mass index: a genome-wide analysis, *Lancet* 383 (2014) 1990–1998.
- [12] J. Adamski, Genome-wide association studies with metabolomics, *Genome Med.* 4 (2012) 34.
- [13] C.B. Newgard, J. An, J.R. Bain, M.J. Muehlbauer, R.D. Stevens, et al., A branched-chain amino acid-related metabolic signature that differentiates obese and lean humans and contributes to insulin resistance, *Cell Metab.* 9 (2009) 311–326.
- [14] S.J. Mihalik, S.F. Michaliszyn, J. de las Heras, F. Bacha, S. Lee, et al., Metabolomic profiling of fatty acid and amino acid metabolism in youth with obesity and type 2 diabetes: evidence for enhanced mitochondrial oxidation, *Diabetes Care* 35 (2012) 605–611.
- [15] S. Wahl, Z. Yu, M. Kleber, P. Singmann, C. Holzapfel, et al., Childhood obesity is associated with changes in the serum metabolite profile, *Obes. Facts* 5 (2012) 660–670.
- [16] K.L. Spalding, E. Arner, P.O. Westermark, S. Bernard, B.A. Buchholz, et al., Dynamics of fat cell turnover in humans, *Nature* 453 (2008) 783–787.
- [17] E.E. Kershaw, J.S. Flier, Adipose tissue as an endocrine organ, *J. Clin. Endocrinol. Metab.* 89 (2004) 2548–2556.
- [18] E.D. Rosen, B.M. Spiegelman, Adipocytes as regulators of energy balance and glucose homeostasis, *Nature* 444 (2006) 847–853.
- [19] S. de Ferranti, D. Mozaffarian, The perfect storm: obesity, adipocyte dysfunction, and metabolic consequences, *Clin. Chem.* 54 (2008) 945–955.
- [20] X. Guo, K. Liao, Analysis of gene expression profile during 3T3-L1 pre-adipocyte differentiation, *Gene* 251 (2000) 45–53.
- [21] S.E. Ross, R.L. Erickson, I. Gerin, P.M. DeRose, L. Bajnok, et al., Microarray analyses during adipogenesis: understanding the effects of Wnt signaling on adipogenesis and the roles of liver X receptor alpha in adipocyte metabolism, *Mol. Cell Biol.* 22 (2002) 5989–5999.
- [22] N. Billon, R. Kolde, J. Reimand, M.C. Monteiro, M. Kull, et al., Comprehensive transcriptome analysis of mouse embryonic stem cell adipogenesis unravels new processes of adipocyte development, *Genome Biol.* 11 (2010) R80.
- [23] H. Molina, Y. Yang, T. Ruch, J.W. Kim, P. Mortensen, et al., Temporal profiling of the adipocyte proteome during differentiation using a five-plex SILAC based strategy, *J. Proteom. Res.* 8 (2009) 48–58.
- [24] G.I. Welsh, M.R. Griffiths, K.J. Webster, M.J. Page, J.M. Tavaré, Proteome analysis of adipogenesis, *Proteomics* 4 (2004) 1042–1051.
- [25] F. Ye, H. Zhang, Y.X. Yang, H.D. Hu, S.K. Sze, et al., Comparative proteome analysis of 3T3-L1 adipocyte differentiation using iTRAQ-coupled 2D LC-MS/MS, *J. Cell Biochem.* 112 (2011) 3002–3014.
- [26] L.D. Roberts, S. Virtue, A. Vidal-Puig, A.W. Nicholls, J.L. Griffin, Metabolic phenotyping of a model of adipocyte differentiation, *Physiol. Genomics* 39 (2009) 109–119.
- [27] C. Gieger, L. Geistlinger, E. Altmaier, M. Hrabce de Angelis, F. Kronenberg, et al., Genetics meets metabolomics: a genome-wide association study of metabolite profiles in human serum, *PLoS Genet.* 4 (2008) e1000282.
- [28] T. Illig, C. Gieger, G. Zhai, W. Romisch-Margl, R. Wang-Sattler, et al., A genome-wide perspective of genetic variation in human metabolism, *Nat. Genet.* 42 (2010) 137–141.
- [29] K. Suhre, S.Y. Shin, A.K. Petersen, R.P. Mohney, D. Meredith, et al., Human metabolic individuality in biomedical and pharmaceutical research, *Nature* 477 (2011) 54–60.
- [30] Y. Fu, N. Luo, R.L. Klein, W.T. Garvey, Adiponectin promotes adipocyte differentiation, insulin sensitivity, and lipid accumulation, *J. Lipid Res.* 46 (2005) 1369–1379.
- [31] S. Rozen, H. Skaletsky, Primer3 on the www for general users and for biologist programmers, *Methods Mol. Biol.* 132 (1999) 365–368.
- [32] K.J. Livak, T.D. Schmittgen, Analysis of relative gene expression data using real-time quantitative PCR and the 2<sup>-</sup>(Delta Delta C(T)) Method, *Methods* 25 (2001) 402–408.
- [33] J.E. Kugler, M. Horsch, D. Huang, T. Furusawa, M. Rochman, et al., High mobility group N proteins modulate the fidelity of the cellular transcriptional profile in a tissue- and variant-specific manner, *J. Biol. Chem.* 288 (2013) 16690–16703.
- [34] M. Horsch, S. Schädler, V. Gailus-Durner, H. Fuchs, H. Meyer, et al., Systematic gene expression profiling of mouse model series reveals coexpressed genes, *Proteomics* 8 (2008) 1248–1256.
- [35] R.D. Stewart, T.A. Duhamel, S. Rich, A.R. Tupling, H.J. Green, Effects of consecutive days of exercise and recovery on muscle mechanical function, *Med. Sci. Sports Exerc* 40 (2008) 316–325.
- [36] A.I. Saeed, V. Sharov, J. White, J. Li, W. Liang, et al., TM4: a free, open-source system for microarray data management and analysis, *Biotechniques* 34 (2003) 374–378.
- [37] V.G. Tusher, R. Tibshirani, G. Chu, Significance analysis of microarrays applied to the ionizing radiation response, *Proc. Natl. Acad. Sci. U. S. A.* 98 (2001) 5116–5121.
- [38] J. Herrero, A. Valencia, J. Dopazo, A hierarchical unsupervised growing neural network for clustering gene expression patterns, *Bioinformatics* 17 (2001) 126–136.
- [39] R. Edgar, M. Domrachev, A.E. Lash, Gene Expression Omnibus: NCBI gene expression and hybridization array data repository, *Nucleic Acids Res.* 30 (2002) 207–210.
- [40] W. Römisch-Margl, C. Prehn, R. Bogumil, C. Röhring, K. Suhre, et al., Procedure for tissue sample preparation and metabolite extraction for high-throughput targeted metabolomics, *Metabolomics* 8 (2012) 133–142.
- [41] C. Jourdan, A.K. Petersen, C. Gieger, A. Doring, T. Illig, et al., Body fat free mass is associated with the serum metabolite profile in a population-based study, *PLoS One* 7 (2012) e40009.
- [42] I. Unterwurzacher, T. Koal, G.K. Bonn, K.M. Weinberger, S.L. Ramsay, Rapid sample preparation and simultaneous quantitation of prostaglandins and lipoxygenase derived fatty acid metabolites by liquid chromatography-mass spectrometry from small sample volumes, *Clin. Chem. Lab. Med.* 46 (2008) 1589–1597.
- [43] G. Kastenmüller, W. Römisch-Margl, B. Wägele, E. Altmeier, K. Suhre, Metaparser: a web-based metabolomics data analysis tool, *J. Biomed. Biotechnol.* 2011 (2010) ID839862.
- [44] A.K. Student, R.Y. Hsu, M.D. Lane, Induction of fatty acid synthetase synthesis in differentiating 3T3-L1 preadipocytes, *J. Biol. Chem.* 255 (1980) 4745–4750.
- [45] B. Laxman, D.E. Hall, M.S. Bhojani, D.A. Hamstra, T.L. Chenevert, et al., Noninvasive real-time imaging of apoptosis, *Proc. Natl. Acad. Sci. U. S. A.* 99 (2002) 16551–16555.
- [46] P. Tontonoz, E. Hu, R.A. Graves, A.I. Budavari, B.M. Spiegelman, mPPAR gamma 2: tissue-specific regulator of an adipocyte enhancer, *Genes Dev.* 8 (1994) 1224–1234.
- [47] B.M. Spiegelman, S.R. Farmer, Decreases in tubulin and actin gene expression prior to morphological differentiation of 3T3 adipocytes, *Cell* 29 (1982) 53–60.
- [48] F.M. Gregoire, C.M. Smas, H.S. Sul, Understanding adipocyte differentiation, *Physiol. Rev.* 78 (1998) 783–809.
- [49] J.A. Ortiz, G. Gil-Gomez, R.P. Casaroli-Marano, S. Vilaro, F.G. Hegardt, et al., Transfection of the ketogenic mitochondrial 3-hydroxy-3-methylglutaryl-coenzyme A synthase cDNA into Mev-1 cells corrects their auxotrophy for mevalonate, *J. Biol. Chem.* 269 (1994) 28523–28526.
- [50] S. Balasubramaniam, J.L. Goldstein, M.S. Brown, Regulation of cholesterol synthesis in rat adrenal gland through coordinate control of 3-hydroxy-3-methylglutaryl coenzyme A synthase and reductase activities, *Proc. Natl. Acad. Sci. U. S. A.* 74 (1977) 1421–1425.
- [51] A. Wolk, M. Furuheim, B. Vessby, Fatty acid composition of adipose tissue and serum lipids are valid biological markers of dairy fat intake in men, *J. Nutr.* 131 (2001) 828–833.
- [52] A.S.C. Pereira, M.V.d. Santos, G. Aferri, Corte RRPdS, Silva SdLe, et al., Lipid and selenium sources on fatty acid composition of intramuscular fat and muscle selenium concentration of Nellore steers, *Rev. Bras. Zootec.* 41 (2012) 2357–2363.
- [53] B. Jenkins, J.A. West, A. Koulman, A review of odd-chain fatty acid metabolism and the role of pentadecanoic acid (c15:0) and heptadecanoic acid (c17:0) in health and disease, *Molecules* 20 (2015) 2425–2444.
- [54] T. Kopf, M. Peer, G. Schmitz, Genetic and metabolic determinants of fatty acid chain length and desaturation, their incorporation into lipid classes and their effects on risk of vascular and metabolic disease, in: K. Suhre (Ed.), *Genetics Meets Metabolomics*, Springer New York, 2012, pp. 191–231.
- [55] W. Yang, T. Kelly, J. He, Genetic epidemiology of obesity, *Epidemiol. Rev.* 29

- (2007) 49–61.
- [56] T.J. Wang, M.G. Larson, R.S. Vasan, S. Cheng, E.P. Rhee, et al., Metabolite profiles and the risk of developing diabetes, *Nat. Med.* 17 (2011) 448–453.
- [57] A. Floegel, N. Stefan, Z. Yu, K. Muhlenbruch, D. Drogan, et al., Identification of serum metabolites associated with risk of type 2 diabetes using a targeted metabolomic approach, *Diabetes* 62 (2013) 639–648.
- [58] R. Wang-Sattler, Z. Yu, C. Herder, A.C. Messias, A. Floegel, et al., Novel biomarkers for pre-diabetes identified by metabolomics, *Mol. Syst. Biol.* 8 (2012) 615.
- [59] E. Ferrannini, A. Natali, S. Camastra, M. Nannipieri, A. Mari, et al., Early metabolic markers of the development of dysglycemia and type 2 diabetes and their physiological significance, *Diabetes* 62 (5) (2013 May) 1730–1737, <http://dx.doi.org/10.2337/db12-0707>.
- [60] U. Batista, M. Garvas, M. Nemeč, M. Schara, P. Veranic, et al., Effects of different detachment procedures on viability, nitroxide reduction kinetics and plasma membrane heterogeneity of V-79 cells, *Cell Biol. Int.* 34 (2010) 663–668.
- [61] I. Ishii, Y. Ikeguchi, H. Mano, M. Wada, A.E. Pegg, et al., Polyamine metabolism is involved in adipogenesis of 3T3-L1 cells, *Amino Acids* 42 (2012) 619–626.
- [62] Y.S. Cha, J.S. Eun, S.H. Oh, Carnitine profiles during differentiation and effects of carnitine on differentiation of 3T3-L1 cells, *J. Med. Food* 6 (2003) 163–167.
- [63] J. Rosenthal, A. Angel, J. Farkas, Metabolic fate of leucine: a significant sterol precursor in adipose tissue and muscle, *Am. J. Physiol.* 226 (1974) 411–418.
- [64] U. Wendel, Abnormality of odd-numbered long-chain fatty acids in erythrocyte membrane lipids from patients with disorders of propionate metabolism, *Pediatr. Res.* 25 (1989) 147–150.